

# An investigation about thin films of poly[2-methoxy-5-(2'-ethyl-hexyloxy) phenylene vinylene] (MEH-PPV) prepared by Langmuir-Schaefer technique

M. K. RAM\*

*Polo Nazionale Bioelettronica, Genoa Section, Corso Europa 30, 16132 Genoa, Italy*

P. BERTONCELLO†

*Department of Chemistry and Biochemistry, The University of Texas at Austin, 1 University Station, MailStop A5300, Austin, TX 78712, USA*

*E-mail: pbertonc@cm.utexas.edu*

C. NICOLINI

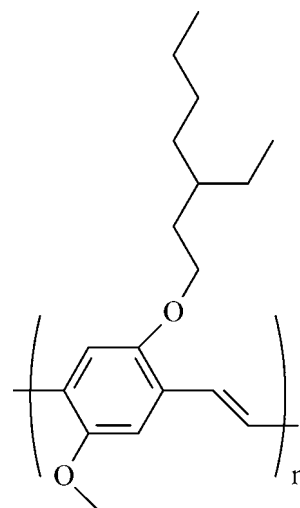
*Department of Biophysical, M&O Science and Technologies (DI.S.T.BI.M.O.), University of Genoa, Corso Europa 30, 16132 Genoa, Italy*

The Langmuir monolayer behaviour of poly[(2-methoxy-5-(2'-ethyl-hexyloxy) phenylene vinylene] (MEH-PPV) conducting polymer was investigated at air-water interface at different subphases containing anions. A uniform deposition of MEH-PPV monolayers was shown by UV-visible, electrochemical techniques, where the influence of anions on redox properties was investigated by cyclic voltammetric surveying. The nature of anions revealed significant changes in redox properties of the MEH-PPV LS films. The photoelectrochemical response of MEH-PPV LS conducting polymer was also investigated at length. © 2003 Kluwer Academic Publishers

## 1. Introduction

The technological capabilities to manipulate matter under controlled conditions, and in order to assemble supramolecular complex structures within the range of 100 nm, can allow the achievement of innovative nano-devices based on non-conventional photovoltaic materials, namely conducting polymers, fullerenes, phthalocyanines and as well related composites materials [1–5]. Among various conducting polymers, aromatic-conducting polymers such as polythiophene, poly(p-phenylene vinylene), poly(p-phenylene), polyaniline, poly(phenylene sulphide) and their derivatives have been used as photoconductive materials [6–12]. Poly(phenylene vinylene)s (PPVs) are main-chain conjugated polymers, which reveal interesting electrical and photo-conjugated properties, and make them suitable for opto-electronics and microelectronics devices [13–18]. Specifically, in recent years, the mechanisms of charge-carrier generation in PPVs and their photoconductivity have been intensely researched in solution and solid films, respectively [17, 18]. The poly[2-methoxy-5-(2'-ethyl-hexyloxy) phenylene vinylene] (MEH-PPV, see Schematic 1) is an important member of PPVs family because of its excellent processibility and favorable electronic and spectroscopic

properties [19–22]. The MEH-PPV is an asymmetrically substituted PPV derivative and it has been found to improve solubility in a range of solvents that shows the low oxidation potential than parent PPVs [23–31]. Recently, we adopted a modified Gilch route for the synthesis of MEH-PPV conducting polymer, which was soluble in most of the common organic solvents [25].



Schematic 1 shows formula structure of MEH-PPV molecule.

\* Present address: Fractal Systems Inc., 200 9th Avenue North, Suite 100 Safety Harbor, FL 34695, USA.

† Author to whom all correspondence should be addressed.

Langmuir-Blodgett or layer-by-layer techniques offer one of the few means for the preparation of ordered systems with molecular architectures where thickness is controllable to a molecular level [26–31]. The recent past has shown the fabrication of Langmuir-Blodgett films of precursors of PPVs class of materials. The PPVs LB films were prepared by heat treatment of a precursor polymer consisting of poly(sulfonium) salt with or without long chain perfluoro-alkyl or a bilayer forming amphiphile as counter ions [32–36]. The heat treatment causes a severe disruption to the large fraction of the film structure. Due to solubility of MEH-PPV in volatile organic solvent an attempt was made to deposit directly the Langmuir-Schaefer (LS) films of MEH-PPV conducting polymer. The Langmuir isotherms of MEH-PPV were studied at air-water interface using various electrolytes. The manufactured LS films were characterized by using UV-visible, FTIR and electrochemical techniques, respectively. We used the measurements of electrochemical photocurrent as a sensitive technique to separate the effects of water from those of oxygen on the whole of the polymer films. The electrochemical photo-response of MEH-PPV LS films in various electrolytic media was also studied. The photoelectrochemical response behaviour of MEH-PPV LS films were measured and compared, respectively.

## 2. Experimental section

### 2.1. Materials

Different substrates were used in this study, mainly indium tin oxide (ITO) obtained from Delta Technologies Ltd. (USA) with  $R_s = 8\text{--}12 \Omega$  (used for electrochemical measurements), quartz slides and cuvettes obtained from Hellma (Germany) for optical absorption measurements. All substrates were cleaned with chloroform and acetone before the film deposition. All chemicals utilized were of analytical grade quality and purchased from Sigma-Aldrich.

### 2.2. Synthesis of MEH-PPV

The synthesis of MEH-PPV is carried out based on our previous work utilizing the modified Gilch route [26]. The proposed modified Gilch synthetic route was followed by functional PPV using alkoxy group as a side chain. Initially, the monomer such as 4-(2'-ethylhexyloxy) anisole and 1,4-Bis (Chloromethyl)-2-(2'-ethylhexyloxy)-5-methoxybenzene were synthesized and later, such monomer was polymerized to obtain MEH-PPV conducting polymer. The product yield was 60%. The obtained MEH-PPV powder was stored under nitrogen atmosphere. The resulting polymer was soluble in chloroform and benzene

### 2.3. Fabrication of Langmuir-Schaefer films of MEH-PPV

The homogeneous solution of MEH-PPV polymer was obtained in chloroform at 1 mg/ml by sonicating for two hours. The resulting solution was filtered using a 0.5  $\mu\text{m}$  filter. The MEH-PPV Langmuir monolayer was formed by using Langmuir trough (MDT corporation,

Moscow, Russia—240 mm  $\times$  100 mm). The effect of anions on the formation of Langmuir monolayer was investigated at the air-water interface for the subphases containing different electrolytes, i.e., pure water,  $\text{FeCl}_3$ ,  $\text{H}_2\text{SO}_4$  and  $\text{NaCl}$ , respectively. The LS films of MEH-PPV were deposited at a surface pressure of 14 mN/m. In fact, the deposition of precursor of the substituted PPVs is shown at surface pressure of 15 mN/m [34].

### 2.4. Optical measurements

The UV-visible spectra of MEH-PPV LS films deposited on glass as well as quartz substrates were recorded by using the UV-visible spectrophotometer (Jasco model 7800).

### 2.5. FTIR measurements

The vibrational bands of MEH-PPV LS films deposited on (111) single crystal of silicon was measured using FTIR spectrophotometer (Bruker, model Vectra V22). The sample chamber was continuously purged with nitrogen gas for 20 min before data collection, and during the measurements to eliminate water vapour absorption. For each sample, 60 interferograms were recorded, averaged and Fourier-transformed to produce a spectrum with nominal resolution of 4  $\text{cm}^{-1}$ . The FTIR spectra of silicon with/without LS films were measured in transmission mode. FTIR spectra of MEH-PPV LS films were obtained after proper subtraction with recorded silicon baseline.

### 2.6. Electrochemical and photochemical measurements

The electrochemical measurements were made by Potentiostat/Galvanostat (EG&G PARC, model 263A) with a supplied software (M270). A standard three electrodes configuration was used, where LS films of MEH-PPV on ITO coated glass plate acted as a working electrode, platinum as a counter and  $\text{Ag}/\text{AgCl}$  as a reference electrode. The electrochemical experiments were conducted using a relatively working electrode area (24  $\text{mm}^2$ ) in the solution that was employed to investigate the redox behaviours of MEH-PPV LS films. The photoelectrochemical current was measured using a standard cell containing three electrodes. A visible light of 150 W was illuminated keeping a distance of 50 to 100 mm from the working electrode for the photoelectrochemical current response.

## 3. Results and discussion

### 3.1. Langmuir isotherms

Fig. 1 observes the variation in pressure-area isotherms of MEH-PPV molecules at air-water interface at subphases containing either pure water,  $\text{FeCl}_3$ ,  $\text{H}_2\text{SO}_4$  or  $\text{NaCl}$ . The pure water causes a sharp increase in the surface pressure of MEH-PPV molecules in Fig. 1 (curve a) whereas no sharp transition is seen either in  $6 \times 10^{-3}$  M  $\text{FeCl}_3$  or 0.1 M  $\text{NaCl}$  subphase solutions (Fig. 1, curve b and d). At the low concentration of the salt, the charged groups of the polymer repel each other, and the polymer

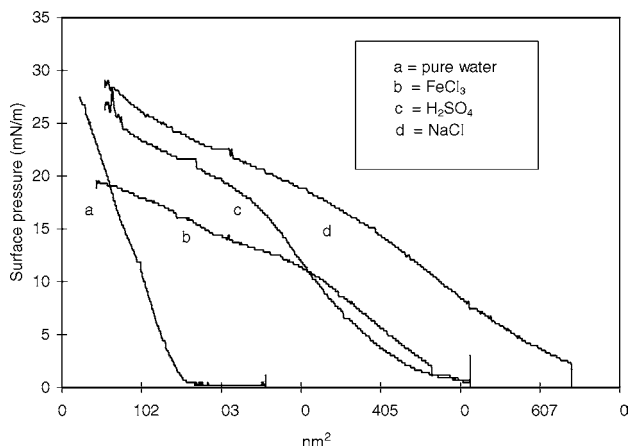


Figure 1 Variation of pressure-area isotherm as a function of electrolytes: (a) pure water, (b)  $6 \times 10^{-3}$  M  $\text{FeCl}_3$ , (c)  $\text{H}_2\text{SO}_4$ , (pH 2) and (d) 0.1 M NaCl.

adopts an extended conformations [23]. The subphase containing  $\text{H}_2\text{SO}_4$  acid (pH 2) maintains a sharp phase transition in the pressure-area isotherm between 1 and 18 mN/m, but further compression slows down the surface pressure of the monolayer. The coil structure of the polymer changes differently at various ionic strength containing solutions, indicating the opening of MEH-PPV chain structure at  $\text{H}_2\text{SO}_4$  acid (pH 2) at air-water interface.

A smooth phase transition depicted at 10–12 mN/m shows an increase in surface pressure and closely interacts by increasing the 2D packing degree of MEH-PPV molecules during solid phase transition. The polymer molecules show maximum 18 mN/m area/molecule near at a surface pressure [19–27]. An increase in any surface pressure reveals 3D transformation at 25–29 mN/m, namely a collapse pressure. The extrapolated area per each repeating unit at solid phase transition is estimated to be  $0.16 \text{ nm}^2$  [27], indicating that aromatic rings and the methoxy groups of the polymer lie flat at the air-water interface. The recent trend of literatures also confirms that aromatic ring containing methoxy group occupies  $0.18$  to  $0.20 \text{ nm}^2$  area/molecule, whereas we observed  $0.16 \text{ nm}^2$  at air-water interface [33]. The area/molecule was estimated to be  $0.16$ ,  $0.40$ ,  $0.48$  and  $0.65 \text{ nm}^2$  for various subphases containing pure water,  $\text{FeCl}_3$ ,  $\text{H}_2\text{SO}_4$  and NaCl, respectively (see Table I). Based on the result of area/molecule obtained in pure water, which is close proximity to the literature trend, an attempt has been made to deposit MEH-PPV molecule using this subphase. The Langmuir-Schaefer films have also been deposited at a subphase containing  $\text{H}_2\text{SO}_4$  for comparison purposes.

TABLE I Area per molecule of MEH-PPV obtained in different subphases

Subphase	Area/molecule ( $\text{nm}^2$ )
$\text{H}_2\text{O}$	0.16
$6 \times 10^{-3}$ M $\text{FeCl}_3$	0.40
$\text{H}_2\text{SO}_4$ (pH 2)	0.48
0.1 M NaCl	0.65

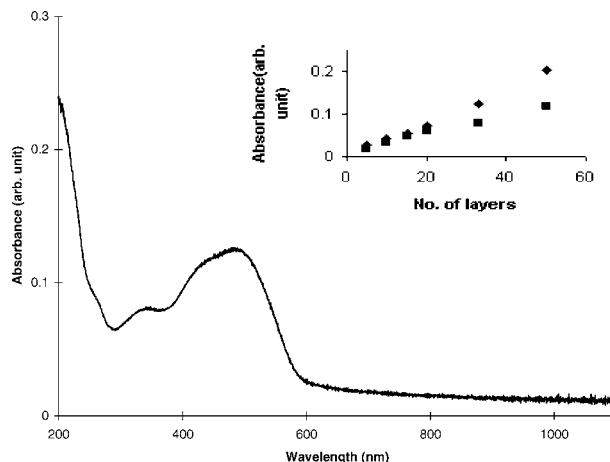


Figure 2 UV-vis spectra of 20 layers MEH-PPV LS films on quartz plate; Inset shows the UV-visible absorption magnitudes at 425 nm (■) and at 324 nm (◆) as a function of layers.

### 3.2. Optical/surface studies

The attempt was made to understand the effect of solvent on the absorption bands of MEH-PPV molecule. We made to dissolve MEH-PPV synthesized molecules on different solvents and the respective UV-vis spectrum was measured in the solution phase. Table I shows the UV-Vis bands obtained in different solvents. The UV-vis absorption has been minimum in chloroform whereas solution shows the blue shift in the absorption band of MEH-PPV. We have tried to fabricate LS films of MEH-PPV using chloroform which acts as plasticizer and helps in fabrication of monolayer. Fig. 2 depicts the UV-vis spectra of 33 layers MEH-PPV LS films that reveal peaks at 477 and 217 nm, and two weaker peaks at 324 and 259 nm, respectively. The absorption at 477 nm is ascribed to  $\pi$ - $\pi^*$  transition of the MEH-PPV polymer and shoulder in absorption is related to the packing effects in of MEH-PPV LS films. The peak at 220 nm arises due to highly localized states originating from the molecular orbital of the benzene transition. The peak at 259 nm is the subject of debate and workers claim that the transition arises because of finite size effects arising from structural disorder. The  $\pi$ -electron system of the polymer consists of segments with a distribution of conjugation lengths. The inset in Fig. 2 shows the absorption magnitudes at 477 and 324 nm as a function of layers, and the observed linearity shows uniform deposition in MEH-PPV LS film. The absorption magnitude was found to be less as compared to solution revealing that the water might be changing the orientation or structure when the molecules are spread on air-water interface for Langmuir monolayer (as shown in Table II).

TABLE II The maximum of absorption of MEH-PPV in different solvent

Solvent	$\pi$ - $\pi^*$ in solvent	$\pi$ - $\pi^*$ in LS films in nm
Chloroform	477	470
THF	485	–
Benzene	495	490
Chlorobenzene	494	–
$\text{CH}_2\text{Cl}_2$	493	–

TABLE III The FTIR bands of MEH-PPV LS films

FTIR band of LS film in wavenumber ( $\text{cm}^{-1}$ )	Peak assignments
3050	CH-Stretching vinyl
2954	$\text{CH}_3$ asymmetric stretching
2918	CH-stretching
2849	$\text{CH}_2$ stretching
1755	Formation of aromatic aldehydes
1601	Aromatic stretching
1502	Semicircular phenyl stretch (C-C aromatic)
1458	Antisymmetric phenyl stretch
1410	Semicircular phenyl stretch
1347	Symmetric alkyl $\text{CH}_2$ deformation
1201	Phenyl oxygen stretch
1035	Alkyl oxygen stretch
957	Trans double bond CH-wag (vinyl group)
835	Out of plane phenyl CH-wag
776	Out of plane ring bend of phenyl ring

The FTIR measurements of several MEH-PPV films on (111) single crystalline surface were performed. FTIR spectra of 300 monolayers of MEH-PPV LS films are shown with proper subtraction of the silicon base line as shown in Table III. It shows the characteristics peaks of MEH-PPV polymer besides the appearance of the band at  $1755 \text{ cm}^{-1}$  suggesting the formation of aromatic aldehydes. Due to the long chain solubilizing side groups, the films of MEH-PPV are expected to be much softer than those of the parent polymer poly(p-phenylene vinylene) (PPV).

### 3.3. Electrochemical study

Fig. 3 depicts the cyclic voltammograms of 10 layers MEH-PPV LS films in different electrolytes vis: 0.1 M HCl, 0.1 M KCl, and 0.1 M TBATFB (tetrabutylammoniumtetrafluoroborate). Different redox potentials have been observed for MEH-PPV molecules for each electrolyte. The CV of MEH-PPV LS films in 0.1 M HCl (Fig. 3a) reveals a strong redox peak potential at  $-262 \text{ mV}$  vs Ag/AgCl. The CV in KCl (Fig. 3b) does not clearly indicate the oxidation process. It seems difficult to determine the onset potential of the redox process using KCl as an electrolyte. The CV of MEH-PPV in acetonitrile containing 0.1 M TBATFB (Fig. 3c) observes redox processes indicate slower movement of the TBATFB ions. The magnitude of current observed in CV is smaller indicating lower conductivity in the presence of TBATFB electrolyte. The higher operating voltage in MEH-PPV system can be attributed to the lower value of ionic conductivity. The slow ionic motion does not favour electrochemical doping at the electrodes and it is not surprising that higher operating voltages are observed for the redox potential. The ionic conductivity increases for the electrolyte as paratoluensulphonic acid (PTS) in Fig. 4. The shape of the cyclic voltammogram (CV) in Fig. 4 reveals the surface confined species and diffusion-controlled system. The redox current magnitude in CV using PTS shows the two orders higher than TBATFB electrolytic system. The redox peak current scale linearly increases with the sweep rate indicating the diffusion controlled system [20].

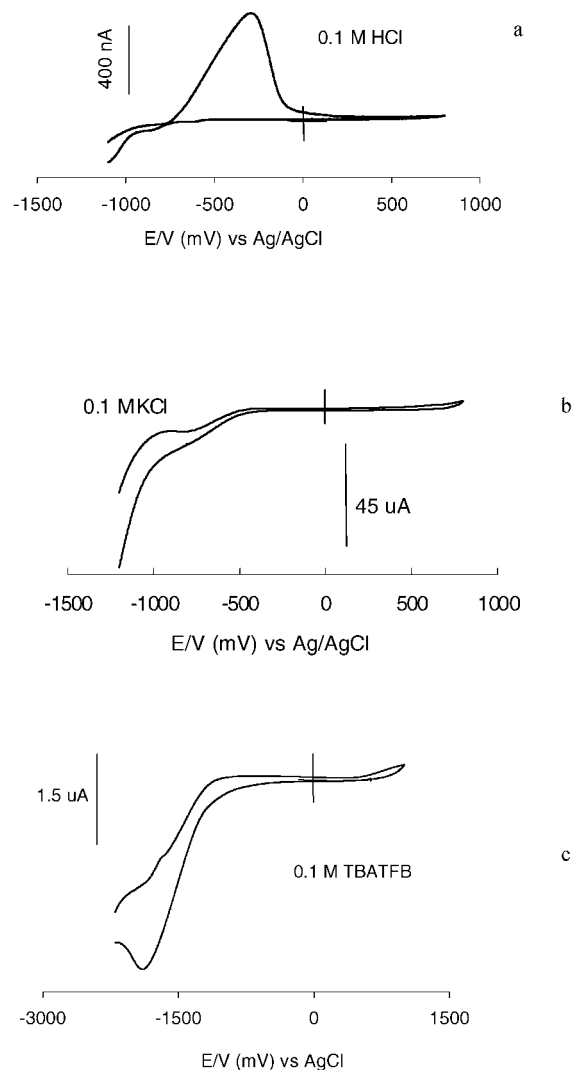


Figure 3 Cyclic voltammograms of 10 monolayers MEH-PPV LS films in different electrolytes: (a) 0.1 M HCl, (b) 0.1 M KCl and (c) 0.1 M TBATFB acetonitrile solution; scan rate 50 mV/s.

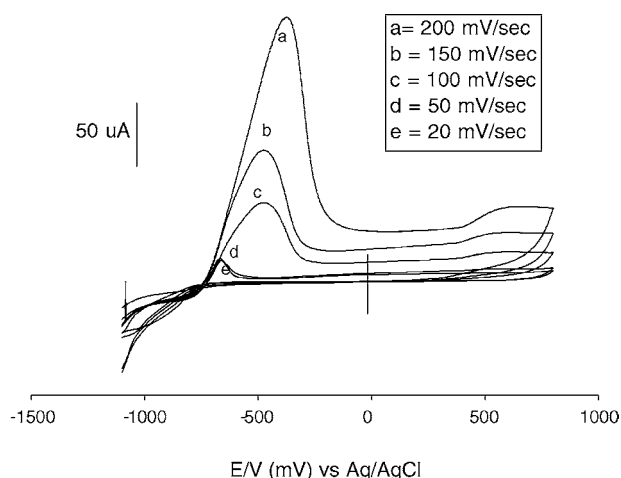


Figure 4 Cyclic voltammograms of 10 monolayers MEH-PPV LS films in 0.1 M PTS at different scan rates: (a) 200 mV/s, (b) 150 mV/s, (c) 100 mV/s, (d) 50 mV/s and (e) 20 mV/s.

### 3.4. Electrochemical photocurrent study

In evaluating the performance of the MEH-PPV in the real system the photoelectrochemical studies are performed by applying a DC potential in a cell containing a two electrode system (platinum as counter and LS films

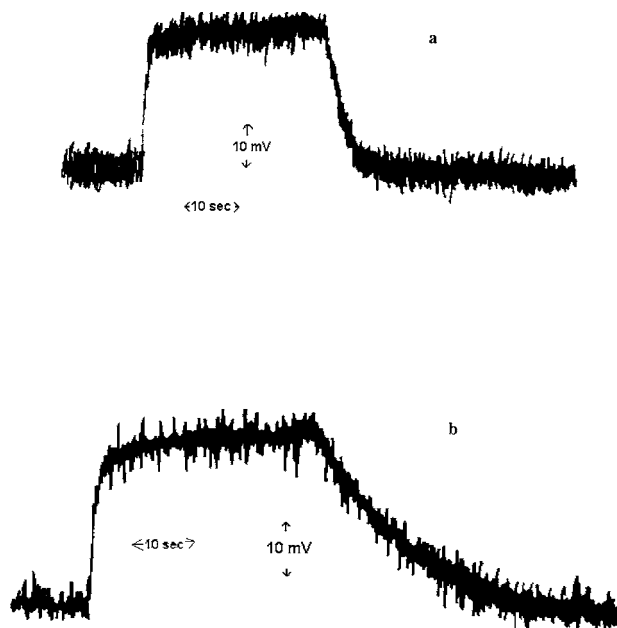


Figure 5 The photoelectrochemical current vs. time (due to oscilloscope there is drop of potential over a load resistance 100 ohm and y axis each unit is 10 mV) for the LS film in 0.1 M TBATFB: (a) zero bias and (b) -1.5 V.

on ITO coated glass plate as working), and applying a white light such that the output is coupled to an oscilloscope that is interfaced to computer. It is focussed on the aspects mentioned above viz. (1) switching time; (2) the dependence of the switching time on ion transport, and in turn is controlled by the ionic composition; (3) the voltage required to be applied to the cell for studying the photoelectrochemical current. The mechanism of MEH-PPV photochemical switching has been extensively investigated at each potential. Fig. 5a shows the photocurrent transient at zero applied potential. The current rising time is faster than the decaying photochemical current time. Fig. 5b there is marked difference in rising and decaying time of MEH-PPV for the applied potential in the cell.

To understand the photocurrent spectroscopy, a 30W visible lamp served as a source as whole wavelength passed through ITO/MEH-PPV side on an electrochemical cell. The steady state electrochemical photocurrent was observed applying potential from 263 A Potentiostat at fixed bias, and the photocurrent was measured. We waited 200 s either for a fixed bias or without a bias in each for recording of photocurrent, and also checked the stabilized photocurrent. To elucidate the role of hole trapping in the process of photo-generation charge separation in various MEH-PPV electrodes, various electrolytes have been used. The uniform photocurrent has been observed in each switch-on and switch-off mode either the electrode containing LS or solution cast films. The photoelectron study has shown that the presence of active-species in the solution exert significantly more appreciably, and spectral distribution of photocurrent. The photocurrent vs. bias is shown in Fig. 6. The depletion layer in the film is practically absent in MEH-PPV due to no external applied bias. The photocurrent is dependent on the applied potential for the wide range of the bias, and starts to change sharply near the on-

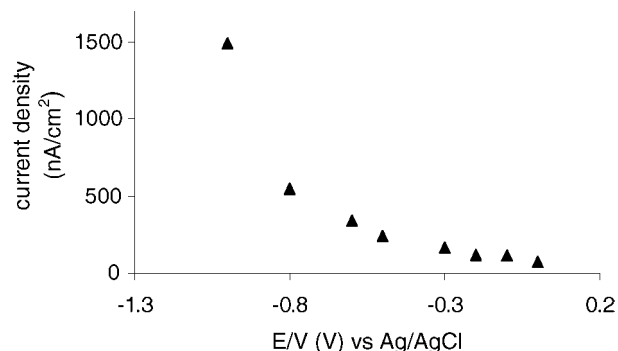


Figure 6 The photoelectrochemical current for the MEH-PPV conducting polymer (30 layers) vs. bias potential (obtained using a standard electrochemical system).

set potential. This is supported by analysis of the dependencies of photocurrent on the electrodes potential. Under the illumination of light to the film, a net positive space charge is expected to form that impairs the current flow. Under illumination by the light longer than the wavelength ( $h\nu > E_g$ ), the effect is maintained more slightly. The phenomenon (the influence of a electrochemical photo current in the dark) may be related to the dark oxidation of the reduced forms of MEH-PPVs, which is accumulated on the electrode surface due to the reduction of adsorbed ions by photoelectron of this conjugated polymer. The slow photocurrent transients are probably associated with the consumption in the interior of MEH-PPV film. This effect is called the trapping of many electrons, photo generated in MEH-PPV by ions. The anions in turn can act as an efficient photoelectron acceptor. After switching the external bias the photocurrent intensity increases gradually and approximately saturates after 200 s. Afterwards it decreases slowly with time for the change of bias with time. The photocurrent intensity decreases immediately to a lower level. It reveals that the MEH-PPV LS films can sustain for bias potential as compared to cast film. This supports the idea that an understanding of the transient behaviour of photoelectrochemical cell solely depends on the consideration of ions motion but needs to take into account the interaction of the injected charges and the ionic space charge field.

#### 4. Conclusions

The types of anions have been found to effect the orientation of MEH-PPV molecules at air-water interface. The minimum area/molecule ( $0.16 \text{ nm}^2$ ) has been observed for pure water as compared to  $0.18\text{--}0.20 \text{ nm}^2$  reported in the literature. A uniform deposition of monolayers was shown by optical and electrochemical techniques. This work focused on the influence of nature of the electrolyte, applied potential and on the electrochemical characteristics of MEH-PPV films. The photoelectrochemical behaviour on LS films of MEH-PPV was found to dependent applied potential. Under the bias the photocurrent is largely dependent on the effect of oxygen rather than water. At present we are using the mixed monolayers of MEH-PPV and fullerene for photovoltaic applications.

## Acknowledgements

Authors are thankful to Dr. N. Sarkar for the synthesis of MEH-PPV conducting polymer and to Mr. A. Baldan, University of Venice, for FTIR measurements. Financial supports from Polo Nazionale Bioelettronica and CNR 5% "Nanotechnology" project "LED based on conducting polymers" are gratefully acknowledged. P.B. is grateful to Edison Termoelettrica SpA for his Ph.D. fellowship.

## References

1. A. KRAFT, A. C. GRIMSDALE and A. B. HOLMES, *Angew. Chem. Int. Ed.* **37** (1998) 402.
2. N. S. SARICIFTCI, L. SMILOWITZ, A. J. HEEGER and F. WUDL, *Synth. Met.* **59** (1993) 333.
3. J. H. BURROGHS, D. D. BRADLEY and A. R. BROWN, *Nature* **347** (1990) 539.
4. D. D. BRADLEY, *Curr. Opin. Solid State Mater. Sci.* **1** (1996) 789.
5. M. LIESS, P. A. LANE, Z. H. KAFIFI and Z. V. VARDENY, *Synth. Met.* **84** (1997) 683.
6. B. DULIEU, J. WERY and S. LEFRANT, *J. Bullot, Phys. Rev.* **57** (1998) 9118.
7. S. BARTH, H. BASSLER, T. WEHRMEISTER and K. MULLEN, *J. Chem. Phys.* **106** (1997) 321.
8. U. RAU and R. BRENDEL, *J. Appl. Phys.* **84** (1998) 6412.
9. M. GAO, B. RICHTER, S. KIRSTEIN and H. MOHWALD, *J. Phys. Chem. B* **102** (1998) 4096.
10. M. K. RAM, S. CARRARA, S. PADDEU, E. MACCIONI and C. NICOLINI, *Langmuir* **13** (1997) 2760.
11. *Idem.*, *Thin Solid Films* **302** (1997) 89.
12. M. K. RAM, G. MASCETTI, S. PADDEU, E. MACCIONI and C. NICOLINI, *Synth. Met.* **89** (1997) 63.
13. H. DEHONG, J. YU and P. F. BARBARA, *J. Amer. Chem. Soc.* **121** (1999) 6936.
14. R. N. MARKS, J. J. M. HALLS, D. D. C. BRADLEY, R. H. FRIEND and A. B. HOLMES, *J. Phys.: Condens. Matter* **6** (1994) 1379.
15. M. A. ANGADI and P. GOSZTOLA, *J. Appl. Phys.* **83** (1998) 6187.
16. J. A. DEARO, D. MOSES and S. K. BURATTO, *Appl. Phys. Lett.* **75** (1999) 3814.
17. I. N. KANG, H. K HONG-KU SHIM and T. ZYUNG, *Chem. Mater.* **9** (1997) 746.
18. A. R. BROWN, D. D. C. BRADLEY, J. H. BURROUGHS, R. H. FRIEND, N. C. GREENHAM, P. L. BURN, A. B. HOLMES and A. KRAFT, *Appl. Phys. Lett.* **61** (1992) 2793.
19. F. HIDE, M. A. DIAZGARCIA, B. J. SCHWARTZ and A. J. HEEGER, *Acc. Chem. Res.* **30** (1997) 430.
20. S. J. MARTIN, D. D. C. BRADLEY, P. A. LANE and H. MELLOR, *Phys. Rev. B* **59** (1999) 15133.
21. P. S. DAVIDS, S. M. KOGAN, I. D. PARKER and D. L. SMITH, *Appl. Phys. Lett.* **69** (1996) 2270.
22. S. C. MORATTI, R. CERVINI, A. B. HOLMES, D. R. BAIGENT, R. H. FRIEND, N. C. GREENHAM, J. GRUNER and P. J. HAMER, *Synth. Met.* **71** (1995) 2117.
23. J. G. HAGTING, R. E. T. P. DE VOS, K. SINKOVICS, E. J. VORENKAMP and A. J. SCHOUTEN, *Macromol.* **32** (1999) 3930.
24. I. H. CAMPBELL, D. L. SMITH, C. J. NEEF and J. P. FERRARIS, *Appl. Phys. Lett.* **75** (1999) 841.
25. N. C. GREENHAM and R. H. FRIEND, in a "Semiconductor Device, Physics of Conjugated Polymers," edited by H. Ehrenreich and F. Spaepen, Vol. 49 (Academic Press, San Diego, 1995).
26. M. K. RAM, N. SARKAR, P. BERTONCELLO, A. SARKAR, R. NARIZZANO and C. NICOLINI, *Synth. Met.* **122** (2001) 369.
27. A. J. PAL, T. OSTERGARD, J. PALOHEIMO and H. STUBB, *Appl. Phys. Lett.* **69** (1996) 1137.
28. A. J. PAL, J. PALOHEIMO and H. STUBB, *ibid.* **67** (1991) 3909.
29. J. G. HAGTING, E. J. VORENKAMP and A. J. SCHOUTEN, *Thin Solid Films* **65** (1998) 327.
30. S. J. MARTIN, H. MELLOR, D. D. C. BRADLEY and P. L. BURN, *Opt. Mater.* **9** (1998) 88.
31. S. PADDEU, M. K. RAM and C. NICOLINI, *J. Phys. Chem. B* **101** (1997) 4759.
32. M. K. RAM, N. S. SUNDARESAN and B. D. MALHOTRA, *ibid.* **97** (1993) 11580.
33. J. H. BATTEN and R. S. DURAN, *Macromol.* **31** (1998) 3148.
34. A. C. FOU, O. ONITSUKA, M. FERREIRA and M. F. RUBNER, *Mater. Res. Soc. Symp. Proc.* **369** (1995) 575.
35. H. H. KIM, R. G. SWARTZ, Y. OTA, T. K. WOODWARD, M. D. FEUER and W. L. WILSON, *J. Light-wave Technology* **12** (1994) 2114.
36. C. YANG, G. HE, R. WANG and Y. LI, *J. Electroanal. Chem.* **471** (1999) 32.

Received 18 September 2002  
and accepted 12 August 2003